



UvA-DARE (Digital Academic Repository)

Molecular dynamics guided analysis of *Bacillus subtilis* spore germination mechanisms

Chen, L.

Publication date
2026

[Link to publication](#)

Citation for published version (APA):

Chen, L. (2026). *Molecular dynamics guided analysis of Bacillus subtilis spore germination mechanisms*. [Thesis, fully internal, Universiteit van Amsterdam].

General rights

It is not permitted to download or to forward/distribute the text or part of it without the consent of the author(s) and/or copyright holder(s), other than for strictly personal, individual use, unless the work is under an open content license (like Creative Commons).

Disclaimer/Complaints regulations

If you believe that digital publication of certain material infringes any of your rights or (privacy) interests, please let the Library know, stating your reasons. In case of a legitimate complaint, the Library will make the material inaccessible and/or remove it from the website. Please Ask the Library: <https://uba.uva.nl/en/contact>, or a letter to: Library of the University of Amsterdam, Secretariat, P.O. Box 19185, 1000 GD Amsterdam, The Netherlands. You will be contacted as soon as possible.

6 Germination of *Bacillus* spores by LiCl^{*}

James Wicander¹, John Gorsuch², Longjiao Chen^{3,4}, Rebecca Caldbeck⁵, George Korza¹, Jocelyne Vreede⁴, Stanley Brul², Graham Christie⁵, Peter Setlow^{1**}

¹ Department of Molecular Biology and Biophysics, UConn Health, Farmington, Connecticut, USA

² BiOWiSH Technologies, Cincinnati, Ohio, USA

³ Molecular Biology & Microbial Food Safety, Swammerdam Institute for Life Sciences, University of Amsterdam, Amsterdam, Netherlands

⁴ Computational Chemistry, Van 't Hoff Institute for Molecular Sciences, University of Amsterdam, Amsterdam, Netherlands

⁵ Department of Chemical Engineering and Biotechnology, University of Cambridge, Cambridge, UK

Abstract

Spores of *Bacillus subtilis* have been found to germinate fully when incubated with LiCl, but not with other monovalent or divalent metal cations. *B. megaterium* spores also germinated with LiCl but *B. cereus* spores did not. In *B. subtilis*, the LiCl germination was via activation of spores' GerA germinant receptor (GR), and in *B. megaterium* it was the GerU GR. Notably LiCl germination was much slower than normal physiological germinant triggered GR germination. In *B. subtilis* spores, rates of LiCl germination were increased in spores with a more fluid IM and decreased in spores with a less fluid IM. Importantly, NaCl strongly inhibited LiCl germination of *B. subtilis* spores, much more so than the larger cation in KCl, although neither salt inhibited L-alanine germination via the GerA GR. In addition, Molecular Dynamics simulations showed that Li⁺ exhibited extensive interaction with GerAB via its extracellular loop. Compared to K⁺ under same simulation conditions, less structural fluctuation and little water passage was observed in simulations with Li⁺. These findings increase our understanding of the mechanistic basis of germination of *Bacillus* spores.

^{*} This chapter includes content adapted from a published article: J. Wicander, J. Gorsuch, L. Chen, R. Caldbeck, G. Korza, S. Brul, G. Christie, and P. Setlow. *Germination of Bacillus spores by LiCl*. *J. Bacteriol.* 207, e00510-24 (2025). Section 6.3.5 *In silico* Li⁺ interaction with GerAB presents additional results that expand upon the published study and was independently performed and analysed by the author of this thesis.

6.1 Importance

The ability of some bacteria to form spores upon nutrient starvation confers properties of metabolic dormancy and enhanced resistance to environmental stressors that would otherwise kill vegetative cells. Since spore forming bacteria include several notable pathogens and economically significant spoilage organisms, insight into how spores are stimulated to germinate and form new vegetative cells is important. Here we reveal that relatively high concentrations of the inorganic salt lithium chloride trigger the germination of *Bacillus subtilis* and *Bacillus megaterium* spores by stimulating one of the spores' nutrient receptors, homologues of which are present in both species. This is significant since novel germinants and increased knowledge of the germination process provide opportunities for improved analysis and control of spores in healthcare, food and environmental sectors.

6.2 Introduction

Spores of *Bacillus* species are dormant, resistant and survive for long periods, but can rapidly come back to life in germination^{27,152,153}. The latter process is triggered by physiological germinants, commonly molecules such as amino acids, sugars or purine nucleosides, their presence presumably signalling that spores' environment is conducive for cell growth. The germinants interact with 3-subunit germinant receptors (GRs) present in spore's inner membrane (IM) that are germinant activated ion channels³⁵. GR activation also leads to rapid excretion of the spore cores' large depot (~ 20% of dry wt) of Ca²⁺ in a 1:1 chelate with dipicolinic acid (CaDPA) via IM channels comprised of SpoVA proteins. CaDPA release then triggers completion of spore germination by activating hydrolysis of spores' peptidoglycan cortex by either of two cortex-lytic enzymes (CLEs), CwlJ and SleB, all this with minimal if any requirement for ATP. Notably, there is much applied interest in spore germination, as when spores germinate, they are relatively easy to kill¹⁵³.

The model spore former *Bacillus subtilis* has three GRs, GerA, GerB and GerK²⁷. The GerA GR responds to L-alanine or L-valine, while the GerB and GerK GRs cooperatively trigger germination with a mixture of L-asparagine, glucose, fructose, and K⁺ (AGFK); the other two GRs have no known germinants, although at least one is present in spores IM^{27,154}. In addition, at least the GerA, GerB and GerK GRs are in an IM complex termed the germinosome in which the IM GerD protein acts as a scaffold^{27,48}. There are 1 or 2 germinosomes in *B. subtilis* spores and germinosome formation increases spore germination rates ≥ 10 -fold^{48,153}. GRs can also be activated by hydrostatic pressures of ~ 150 megaPascals. In addition, the GR-independent germinants dodecylamine and high levels of CaDPA act on other components of the germination apparatus, including the multi-SpoVA protein channel for CaDPA release

(dodecylamine) or the CLE CwJ (CaDPA)²⁷. However, the latter two germinants likely have no physiological relevance.

As noted above for AGFK germination, there are a number of examples of stimulatory effects of monovalent cations on spore germination^{27,54,155,156}. There is also one well documented example of spore germination in response to an inorganic salt alone. This is the rapid germination of *Bacillus megaterium* spores by KBr¹⁵⁶, which appears to activate the GerU GR that is also activated by glucose, proline, and to a lesser extent leucine¹⁵⁷. Surprisingly, in an analysis of effects of lithium ions on endospore viability during storage, LiCl was found to cause a moderately rapid loss in viability of spores of a *B. subtilis* strain. This led to testing of the effects of LiCl on *B. subtilis* spores. Interestingly, LiCl was observed to trigger *B. subtilis* spores' germination, a first for *B. subtilis* spores. These observations led to the studies reported in this communication to determine how LiCl triggers *B. subtilis* spore germination and examining the LiCl germination of spores of several other *Bacillus* species. Notable findings in our work were: i) LiCl germination of *Bacillus* spores was via the GerA GR in *B. subtilis* and GerUV in *Bacillus megaterium*; ii) there were major effects of IM fluidity on rates of *B. subtilis* spore germination with LiCl; iii) one mutation in the GerAB subunit, the likely germinant binding subunit⁴⁴, that abolished L-alanine germination also abolished LiCl germination; and iv) NaCl strongly inhibited LiCl germination but KCl much less so, although neither salt inhibited L-alanine germination via GerA. v) In MD simulations, Li⁺ interacted with GerAB more intensively via its extracellular loop, which is not observed in simulations with K⁺ that shows no germination effect to *B. subtilis* spores. We also observed reduced structural fluctuation and little water passage in Li⁺ simulations compared to K⁺ simulations. These results as well as GerAB molecular modelling suggest how Li⁺ may interact with the GerAB.

6.3 Results

6.3.1 *Bacillus subtilis* spore germination with LiCl

A ~ 70% loss in *B. subtilis* wild-type spore viability in 2 weeks, seen when spores were incubated with LiCl at 40°C was surprising. However, a possible explanation is that LiCl was triggering spore germination, as if spores germinate in a relatively nutrient-free environment they slowly die¹⁵⁸. To test if LiCl was indeed triggering spore germination, spores of our standard wild-type (wt) *B. subtilis* strain, PS832, were germinated with 10 to 500 mM LiCl at 40°C and percentages of spore germination were determined (Table 1). While germination with 10 mM LiCl was slow, the rate of germination increased as the LiCl concentration was incrementally increased up to 500 mM, and germination at 40°C was almost complete in 2 d with ≥ 100 mM LiCl. This germination was due to the Li⁺ ion, as other monovalent chloride salts at 100 mM gave no germination, nor did high concentrations of several divalent cations. That it

was the Li⁺ that was triggering germination and not Cl⁻ was shown by the similar germination of *B. subtilis* spores by several other Li⁺ salts (Table 1). Notably there was no spore germination with 100 mM LiCl at 50°C (Table 1) suggesting that the LiCl germination seen at 40°C involves the normal *B. subtilis* GR-dependent germination pathway, as L-valine germination via the GerA GR was also abolished at 50°C (Table 1 and data not shown).

Salts tested	Concentration (mM)	Germination (%) after incubation at 40°C for:			
		0d	1d	2d	5d
NaCl, KCl or CsCl	100	0	1	0	1
MgCl ₂	100	0	1	2	2
CaCl ₂	100	0	4	3	5
LiCl	10	0	35	89	100
LiCl	100	0	70	100	¹
LiCl ²	100	0	0	0	¹
LiCl	250	0	85	100	¹
LiCl	500	0	98	100	¹
LiBr	10	0	41	92	¹
LiBr	100	0	85	¹	¹
Li Acetate	100	0	80	¹	¹
Li ₂ SO ₄	100	0	85	¹	¹
LiCl (PS4498)	10	0	0	¹	¹
LiCl (PS4498)	100	0	1	¹	¹

Table 1. Germination of *B. subtilis* spores with various monovalent and divalent cations*

*Spores of all strains tested were wt PS832 except for PS4498 lacking all GRs and were incubated at 40°C, unless otherwise noted, in 25 mM Tris-HCl (pH 7.4) with ~2x10⁸ spores/ml, and at various times aliquots were examined by phase contrast microscopy and ~100 spores were scored as phase bright (dormant) or phase dark (germinated).

¹Not analyzed; ²incubated at 50°C

6.3.2 Mechanism of *B. subtilis* spore germination with LiCl

To determine the mechanism of the LiCl germination of *B. subtilis* spores, the germination of multiple isogenic strains with mutations in germination proteins was examined (Table 1, Figure. 1A). Notably, the LiCl germination seen with PS832 spores was eliminated in PS4498 spores lacking all five GRs (Table 1), indicating that one or more GRs was giving rise to the LiCl germination. Examination of the germination of spores lacking single GRs (Figure. 1A) showed that the absence of the GerA GR abolished LiCl germination, while the absence of either GRs with no known germinants (YfkQRT or YndDEF) or the GerB or GerK GRs had only small effects on rates of LiCl germination. In addition, all the GR mutant spores, except the one lacking GerA reached ~75% germination in 24 hr, as did wt spores (Figure. 1A). Loss of the GerD protein that forms the scaffold for germinosome formation also greatly

decreased the rate of LiCl germination (Figure. 1A), as also seen for GR-dependent germination⁴⁸ (6). Notably, the L-valine germination of the parental wild-type strain via the GerA GR (Figure. 1C) was much more rapid than the LiCl germination. However, all strains except the one lacking the GerA GR exhibited relatively similar rates of L-valine germination while the absence of GerD slowed the rate of L-valine germination considerably, as expected^{27,48}.

One potential confounding concern about the results in Figure. 1A,C was that all strains used except the wt strain PS832, carried one or more antibiotic resistance markers replacing the gene for the absent GR. Notably, recent work¹⁰⁸ has indicated that the presence of a gene or plasmid carrying antibiotic resistance markers can lead to significant effects on the *Bacillus cereus* spore proteome; this was the case even though antibiotics were not present during cell growth or sporulation, as was the case with spore preparation in the current work. Given these latter reports, we also prepared GR-less strains with no antibiotic markers and again measured LiCl and L-valine germination of the various strains (Figure. 1B, D). Again, there was general similarity between all strains except those lacking GerA in their LiCl and L-valine mediated germination. Thus, it seems very unlikely that the presence of the antibiotic markers in our constructs had significant effects on rates of GR-dependent LiCl or L-valine spore germination.

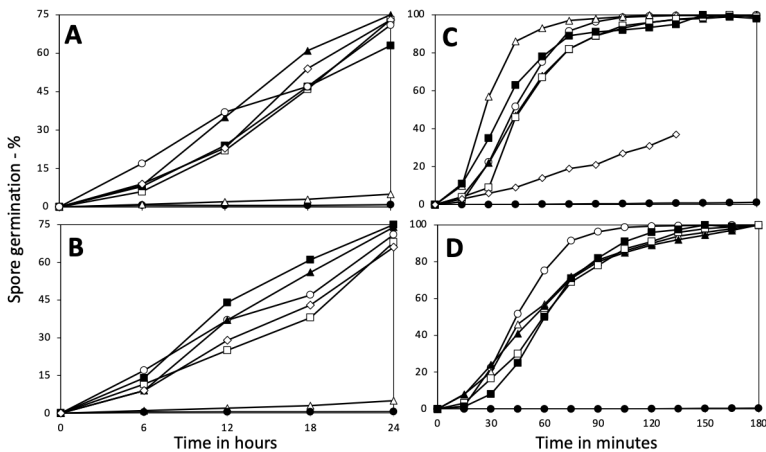


Figure 1. Analysis of effects of deletion mutations with (A, C) or without (B, D) an antibiotic resistance marker, on spore germination with LiCl (A, B) or L-valine (C, D). Spores of various strains were germinated with LiCl or L-valine, and the percentages of spore germination were measured as described in Methods. Symbols of the strains used are: A) ○, PS832 (wt) (this strain has no antibiotic marker); ●, PS4492 ($\Delta gerA$); △, FB62 ($\Delta gerD$); ▲, PS4584 ($\Delta gerKA$); □, PS4585 ($\Delta gerBA$); ■, PS4586 ($\Delta yndD$); and ◇, PS4587 ($\Delta yfkQ$); B) ○, PS832 (wt); ●, PS4589 ($\Delta gerA$); △, FB62 ($\Delta gerD$); this strain does have an antibiotic marker; ▲, PS4590 ($\Delta gerKA$); □, PS4591 ($\Delta gerBA$); ■, PS4592 ($\Delta yndD$); and ◇, PS4593 ($\Delta yfkQ$); C) ○, PS832 (wt) (this strain has no antibiotic marker); ●, PS4492 ($\Delta gerA$); ◇, FB62 ($\Delta gerD$); △, PS4584 ($\Delta gerKA$); ▲, PS4585 ($\Delta gerBA$); □, PS4586 ($\Delta yndD$); and ■, PS4587 ($\Delta yfkQ$); D) ○, PS832 (wt); ●, PS4589 ($\Delta gerA$); △, PS4590 ($\Delta gerKA$); ▲, PS4591 ($\Delta gerBA$); □, PS4592 ($\Delta yndD$); and ■, PS4593 ($\Delta yfkQ$).

Additional factors that can modulate GerA-dependent L-valine germination of *B. subtilis* spores include: i) heat activation by a short incubation at 70°C which can increase rates of L-valine germination by the GerA GR^{27,152,159,44,160}; and ii) spores' IM fluidity, as a) L-valine germination is slowed in spores carrying the 2Duf IM protein which have a less fluid IM than 2Duf-less spores^{44,160} and b) spores lacking three of the five IM homologs of ~75% of 2Duf¹⁶¹ which have elevated IM fluidity¹⁶² germinate significantly faster with L-valine than wt spores (Figure 2A). Notably, while the expected large increase in the rate of L-valine germination was seen in heat activated wt spores (Figure. 2A), heat activation had no observable effect on the rate of LiCl germination (Figure. 2B; and see Discussion). However, the rate of LiCl germination was increased markedly in spores with increased IM fluidity, whether because of the absence of 2Duf, or the absence of multiple homologs of most of 2Duf (Figure. 2B).

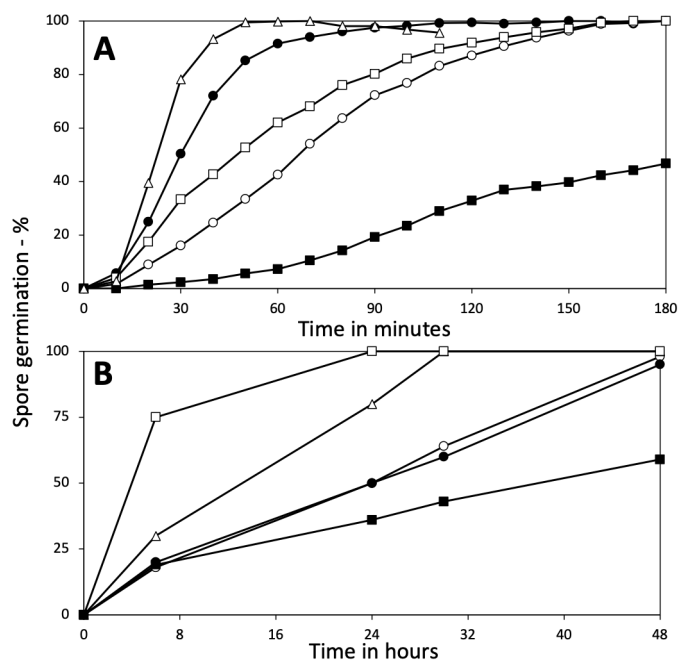


Figure 2. Effects of various mutations or heat activation on *B. subtilis* spore germination with A) L-valine or B) LiCl. Purified spores of various *B. subtilis* strains were germinated in duplicate with or without a heat shock as described in Methods with either: A) L-valine, and percent germination was determined by measurement of dipicolinic acid release and results from duplicate germinations were averaged as described in Methods, or B) 100 mM LiCl, and levels of germination were determined at various times by phase contrast microscopy as described in Methods. All strains are isogenic with strain PS832, except PS4461 and PS4462 that are isogenic with each other. The symbols in A and B) are: ○, PS832 (wt); ●, PS832 (wt) heat activated at 70°C for 30 min; △, PS4531 (lacking three YetF homologs); □, PS4461 (wt); and ■, PS4462, PS4461 plus *spoVA*^{2mob} with the *2duf* gene.

To determine if changes in the likely GerA GR's germinant binding pocket in a putative water channel in the B subunit (GerAB)^{44,45} were involved in facilitating LiCl germination, a *gerAB* point mutant in the putative water channel in this protein¹³⁰ was tested for germination with L-alanine and LiCl (Figure. 3A, B). L-

Alanine was the germinant in this experiment because it was the germinant used to test the effects of these GerAB variants on spore germination¹³⁰. As was recently reported¹³⁰, spores of the GerAB Y97A mutant contained only ~20% of the wt level of the GerAA subunit of the GerA GR. Even so, the GerAB Y97A spores had minimal if any L-alanine germination (Figure. 3A), nor any LiCl germination as well (Figure. 3B). Unfortunately, spores of several other mutants in the putative water channel contained minimal if any GerA GR¹³⁰, so were not used in this work.

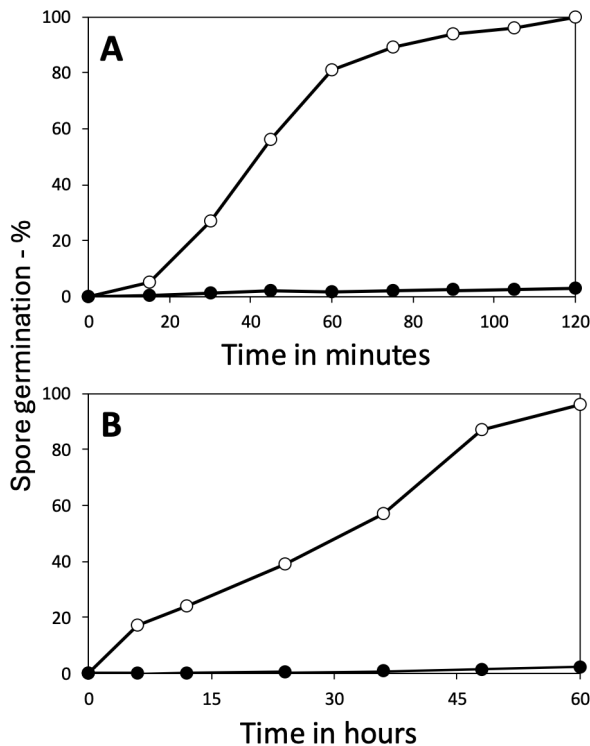


Figure 3. Effects of a *gerAB* mutation on spore germination with A) L-alanine or B) LiCl. Spores of *B. subtilis* PY79 with or without the Y97A mutation in *gerAB* were germinated with either A) L-alanine, or B) LiCl and germination was followed, all as described in Methods. Symbols for the PY79 strains used are: ○, wt, and ●, Y97A. All data are from duplicate germination incubations, and results were averaged as described in Methods.

6.3.3 Influence of other cations on LiCl germination

Optimal conditions for spore germination in aqueous suspensions generally include inorganic salts in addition to the organic germinant compound. In some cases, the germination rate can be influenced by the choice of salt present within the germination buffer. Inosine mediated germination in *Bacillus cereus* spores, for

example, proceeds rapidly in the presence of Na^+ ions but is strongly inhibited in the presence of K^+ ions¹⁶³. With this in mind we decided to investigate whether LiCl germination in *B. subtilis* spores was influenced by the presence of Na^+ or K^+ ions, and if we sought to determine whether the presence of the second cation exerted positive or negative effects on the LiCl germination response. As a control measure, *B. subtilis* PS832 spores were first tested for their germinative response to L-alanine in germination buffer supplemented with either KCl or NaCl, revealing comparable but enhanced germinative rates relative to spores incubated in the non-supplemented germination buffer (Figure 4A). Similarly, LiCl mediated germination appeared to proceed efficiently (>80% germination) in buffer supplemented with 10 mM KCl (Figure 4B). However, NaCl was shown to exert a strong inhibitory effect on LiCl mediated germination, with less than 2% of the spores germinating in LiCl-containing buffer supplemented with 2 mM NaCl over the observed time period (Figure 4B).

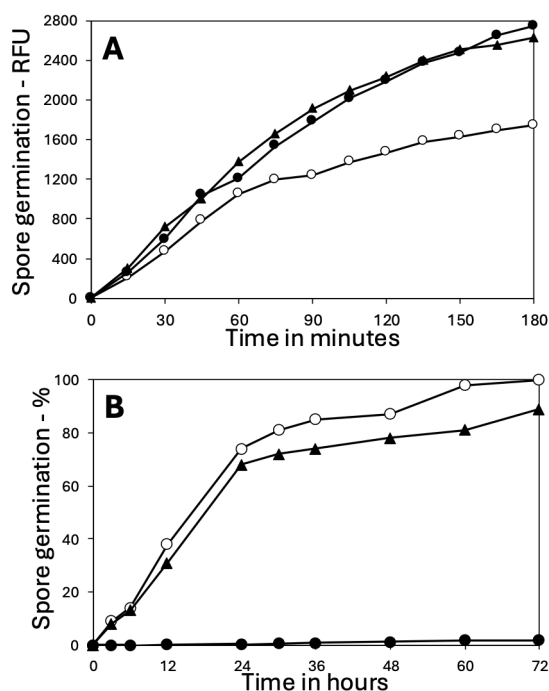


Figure 4. Effects of KCl and NaCl on spore germination with (A) L-alanine or (B) LiCl. A) Spores of PS832 were heat activated and germinated at 37°C with 10 mM L-alanine in 5 mM K-Hepes buffer (pH 7.4) with or without KCl or NaCl, and germination was measured by Tb-DPA fluorescence as described in Methods. The germination was with no additions (○), or with 50 mM KCl (▲) or 10 mM NaCl (●). B) PS832 spores without heat activation were germinated at 40°C in 100 mM LiCl and 5 mM K-Hepes buffer (pH 7.4), and with no additions (○), with 10 mM KCl (▲) or 2 mM NaCl (●).

6.3.4 LiCl-induced spore germination in other *Bacillus* species

Spores of *Bacillus megaterium* and *Bacillus cereus* were also examined to ascertain whether they too germinated in response to aqueous LiCl in order to provide a pointer as to whether this observation extends across the wider Bacillota family. *B. megaterium* PV361 spores germinated in response to LiCl most efficiently when the GerUV germinant receptor was present, but at a slower rate than observed for *B. subtilis* spores; approximately 16% of PV361 pHT:GerUV spores (GC431) were observed to have germinated after 48 hrs in the highest concentration of LiCl tested (250 mM), rising to 60% after 8 days (Table 2). Spores that lacked the GerD protein (GC616) but were otherwise isogenic with strain GC431 showed a reduced rate (30% after 8 days), with further reductions in germinative efficiency in spores lacking either GerUV or all five of the GRs encoded in this species. Notably, the weak germinative response observed in the germinant receptor-less strain (GC614) after 8 days was higher than that observed in the same strain when incubated in 5 mM Tris-HCl buffer alone (17% versus 2%). In general, 250 mM LiCl induced a more efficient germinative response in *B. megaterium* spores than 100 mM LiCl, although a maximal amount of ~ 60% after 8 d was evident under both conditions. In contrast to *B. subtilis* and *B. megaterium*, spores of *B. cereus* 10876 failed to show any germinative response to 250 mM LiCl over 8 days, regardless of whether spores were heat shocked or not prior to incubation (data not shown).

Strain	Concentration (mM) ^b	Germination (%) after incubation at 30°C for:				
		0 h	6 h	24 h	48 h	192 h
PV361	100	0	1	5	6	12
(DgerUV)	250	0	1	1	11	9
PV361 pHT-gerUV	100	0	2	4	13	60
	250	0	3	6	16	58
PV361 DgerD pHT-gerUV	100	0	3	2	3	30
	250	0	2	1	8	30
PV361 ger5	100	0	3	3	6	23
	250	0	4	2	13	17

Table 2. Germination of *B. megaterium* spores with LiCl^a

^a Spores ($\sim 1 \times 10^8$ /ml) were incubated at 30°C in 5 mM Tris-HCl (pH 7.5) containing 100 or 200 mM LiCl, and at various times aliquots were examined by phase contrast microscopy and scored for germination as described in the methods.

^b Control (buffer only) spore germination was <5% in all cases

6.3.5 *In silico* Li⁺ interaction with GerAB

Since GerA is responsible for Li⁺-induced germination in *Bacillus subtilis* and point mutations in the GerAB subunit have been shown to impair this process, we sought to investigate the molecular interactions between Li⁺ and GerAB. We therefore performed molecular dynamics (MD) simulations with either 20 mM LiCl or 20 mM KCl, using KCl as a negative control. K⁺ does not induce germination on its own and

does not compete with Li^+ (compared to Na^+), serving only to maintain the system's neutral charge. For each condition, five parallel 1000-ns simulations were carried out. We first assessed the structural stability of GerAB in the presence of either cation using root-mean-square deviation (RMSD) and root-mean-square fluctuation (RMSF) analyses, calculated based on the carbon alpha (CA) atoms of each residue. RMSD, which reflects overall protein fluctuation as a function of simulation time, stabilized after approximately 200 ns in both conditions (Figure S1), ranging from 0.3nm to 0.5nm Li^+ simulations and ranging from 0.4nm to 0.7nm in K^+ simulations (Figure 5A). This suggests that GerAB shows less structural fluctuation in the presence of Li^+ . RMSF, which reports the average structural deviation of individual residues throughout the whole trajectory, revealed that transmembrane (TM) regions remained generally stable in both conditions. However, loop regions including Extracellular Loop (EL) EL1, EL2, EL3 Intracellular Loop (IL) IL 1 and IL2 exhibited reduced fluctuations in the Li^+ condition ($<0.1\text{nm}$ except for EL3) compared to higher flexibility in the K^+ condition ($>0.1\text{nm}$) (Figure 5B). Slightly reduced fluctuation is also observed for TM regions TM2, TM4, TM5, TM6, TM7 and TM10, with the overall RMSF for all TMs below 0.1nm for both cation conditions. The comparative low RMSD and RMSF shows that the protein is less flexible with the presence of Li^+ than with the presence of K^+ and it is reflected in many regions of the protein.

Next, we analysed ion-protein interactions to determine whether the observed differences in GerAB structural fluctuation could be attributed to specific cation interactions. This was achieved by calculating the minimum distance between each residue and the free ions across all simulation frames. A binding event was defined as the presence of a Li^+ or K^+ ion within 0.4 nm of a given residue in a single frame. The proximity of an ion was defined as the probability of finding a Li^+ or K^+ ion within this cutoff distance throughout the trajectory, where a proximity value of 1 indicates contact in all frames. Although the specific interaction patterns differed between Li^+ (Figure S2) and K^+ simulations (Figure S3), a clear trend emerged showing more persistent interactions in the presence of Li^+ . In K^+ simulations, binding events were transient, typically lasting less than 200ps per interacting residue (Figure S3, A1-E1). In contrast, Li^+ simulations exhibited longer interactions, with some lasting up to 100 ns (Figure S2, A1-E1). Moreover, the total number of binding events in Li^+ simulations was substantially higher, reaching up to 50,000 for certain residues (Figure S2, A2-E2), compared to approximately 20,000 in K^+ systems (Figure S3, A3-E3). This resulted into a significantly higher overall proximity of Li^+ to GerAB residues, with more residues showed more interactions with some reached a maximum proximity value of 1.0 (Figure S2, A3-E3), indicating continuous contact throughout that simulation run. On the contrary, in the K^+ simulation, proximity across the protein was generally lower (around 0.4 with some reaching 0.8) (Figure S3, A3-E3). When comparing average proximity combining the five runs, only two residues in the K^+ condition reached a proximity above 0.4 (Figure 6A). In contrast, 22 residues

exceeding this threshold in the Li^+ condition, with six residues reaching a proximity above 0.9 (Figure 6B). All six high-proximity residues were negatively charged, predominantly glutamic acids, consistent with favourable electrostatic interactions with cations. Notably, these residues were located primarily in extracellular loops, and this distinct binding pattern between GerAB and Li^+ was not observed with K^+ .

These observations led us to examine how the high interaction between Li^+ and GerAB might influence the protein's structural dynamics during simulations. Water permeation was observed in our previous study with K^+ simulations, with up to 121 water passage events per microsecond observed¹⁴⁴, whereas in the presence of Li^+ , this number was drastically reduced to only 1–3 events per microsecond (Figure 7).

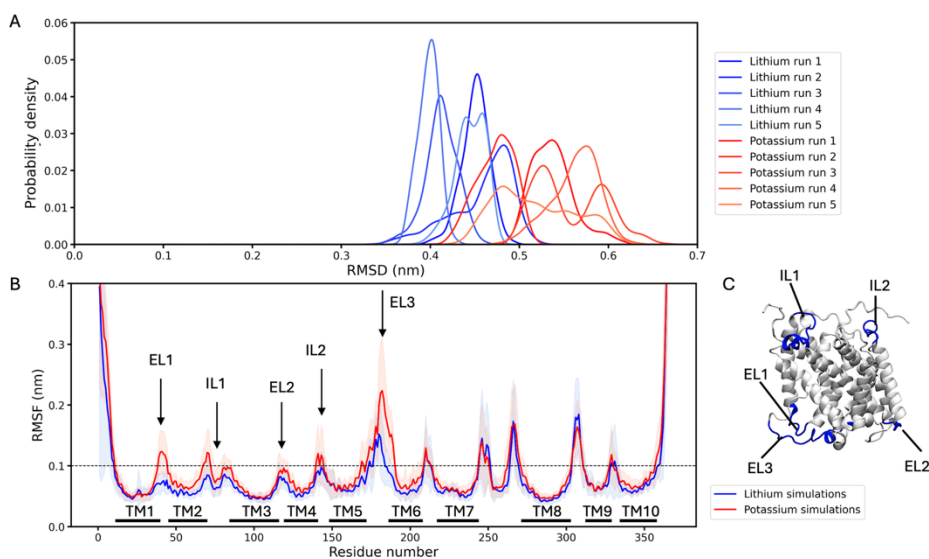


Figure 5. Protein structural fluctuation analysis in MD simulations with the presence of Li^+ or K^+ . (A) Protein CA RMSD for each simulation run with both cation conditions shown in probability density. Since the RMSD increased from 0 to 200ns simulations and stabilized afterwards in all simulation runs (Figure S1), the data before 200ns is excluded. K^+ and Li^+ cation conditions are coloured in different shades of blue and red, respectively. (B) Protein CA RMSF for parallel simulation averaged in each ion condition. Error margin showed \pm std of RMSF for each residue over five runs. K^+ and Li^+ cation conditions are coloured in blue and red, respectively. Black bars marked in the lower figure show the range of TM regions, and black arrows mark the loop regions showing difference in RMSF in the two cation conditions. (C) Snapshot of the GerAB structure with loop regions showing differences in RMSF under two cation conditions, highlighted in blue. The protein is depicted in a New Cartoon representation and coloured in white.

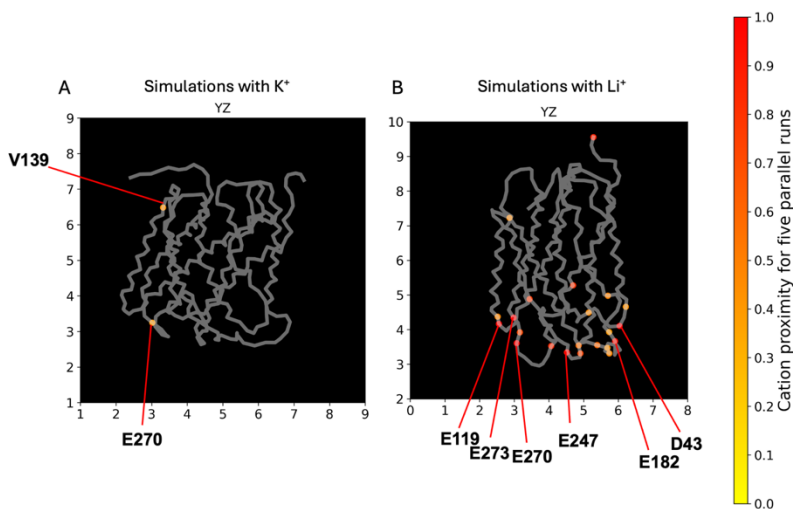


Figure 6. Cation proximity mapped onto the GerAB backbone snapshot across five parallel 1000-ns MD simulations. The last simulation frame of one run was chosen for each cation condition to generate the protein backbone snapshot. In both conditions, the protein was oriented with the N- and C-termini facing upwards with the protein principal axis aligning with the simulation axis perpendicular to the membrane. The termini were assumed to be on the intracellular side of spore IM^{35,105,130}. This locates the intracellular loops at the higher bound of the simulation box and the extracellular loops at the lower bound of the simulation box. (A) K⁺ proximity values projected onto the GerAB structure. Residues with proximity values above 0.4 are color-coded according to the scale bar on the right. (B) Li⁺ proximity values projected onto the GerAB structure. Similarly, residues with proximity values above 0.4 are highlighted and color-coded, and those above 0.9 are labelled.

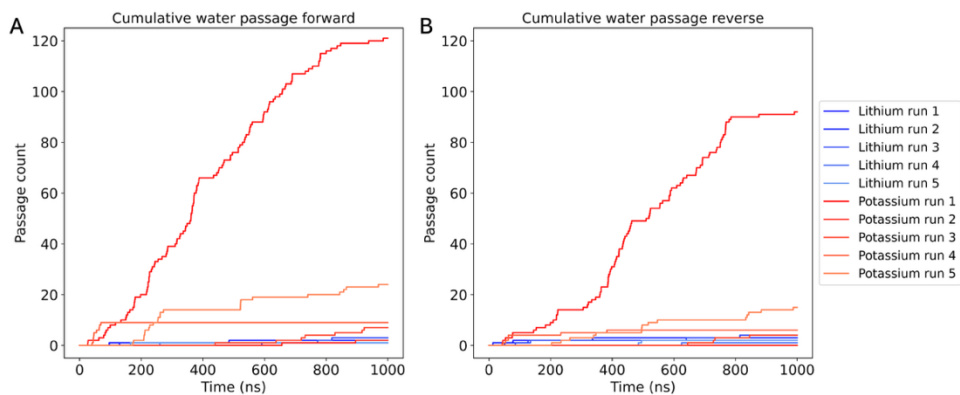


Figure 7. Water passage counts through GerAB in five parallel MD simulations under different ionic conditions. (A) Water passage counts through the “forward” direction of GerAB. (B) Water passage counts through the “reverse” direction of GerAB. Here, “forward” means from the extracellular side to the intracellular side of the membrane. In both panels, K⁺ simulations were coloured in different shades of red while Li⁺ simulations were coloured in different shades of blue.

6.4 Discussion

The finding that LiCl can trigger spore germination in a GR mediated response was surprising as LiCl has not previously been found to trigger *Bacillus* spore germination^{155,156}. LiCl has been shown to be rapidly taken up in *Bacillus thuringiensis* spores' outer layers, and even some into the core, but this was not accompanied by triggering of spore germination¹⁶⁴. In addition, LiCl as well as the salts NaCl, KCl, NH₄Cl, CsCl and RbCl have been shown to stimulate the *B. subtilis* GerA response to L-alanine¹⁶⁵, a response that is much more rapid than with LiCl alone seen in the current work. Thus, the germination of *B. subtilis* spores by LiCl alone via GerA activation is a novel finding, as is the triggering of *B. megaterium* spore germination by LiCl, also by activating a GR in this organism. The question then is how LiCl does this i.e., does it directly activate the appropriate GR by action on these GRs' germinant interaction site, or is it a general effect on the particular GR or even on spore IM structure? In this regard the *B. subtilis* GerA GR is noteworthy, as this GR has been shown to be by far the most sensitive to signals that activate it spontaneously during sporulation, in particular signals that indicate that the sporulation process is not going appropriately¹⁶⁶. GerA-dependent germination via a physiological germinant such as L-valine is also very sensitive to IM fluidity either when: i) the presence of the IM 2Duf protein decreases IM lipid fluidity, or ii) the loss of multiple IM YetF homologs increases IM fluidity, all as seen previously^{161,167} and in this work. Notably, the effects of IM lipid fluidity on LiCl germination were essentially identical to the effects on L-valine germination. In addition, the relative effects of the Y97A mutation in GerAB on L-valine and LiCl germination were similar, suggesting that effects of LiCl are on the GerAB subunit, perhaps facilitating the adoption of a conformation that is more active in triggering germination, including facilitating the release of core monovalent cations which may be how the IM's SpoVA channel for CaDPA release is subsequently activated/opened^{35,168}.

When taking the MD simulation results into account, we observe that Li⁺ interacts more closely with GerAB than K⁺. Increased proximity is observed in the extracellular loop region of GerAB. This coincides with reduced fluctuations in the extracellular loop region of GerAB when Li⁺ is present instead of K⁺, as reflected by RMSF, as well as reduced global protein fluctuations as observed in RMSD. It is therefore possible that Li⁺ stabilizes the protein by interacting with the protein extracellular loop. This observation may provide an explanation for why germination kinetics in the presence of Li⁺ are slower than those triggered by L-alanine, potentially because Li⁺ slows down GerAB-mediated germination by reducing GerAB dynamics. If so, the MD simulation data presented here are not sufficiently informative to provide a mechanistic explanation of how Li⁺ activates GerAB. To verify whether Li⁺ indeed slows down germination kinetics, germination experiments should be performed with both Li⁺ and L-alanine present to determine whether germination remains slowed under these conditions. Furthermore, to gain a better understanding of how Li⁺ triggers GerAB

activation while simultaneously reducing GerAB structural fluctuations, MD simulations of the GerA complex in the presence of Li^+ could be performed in the future. As discussed by the Rudner Group³⁵, GerA is likely to form a pentameric structure composed of GerAA, GerAB, and GerAC trimers. Such simulations may reveal how Li^+ -induced changes in GerAB structural fluctuations affect GerAA and GerAC dynamics, thereby providing more valuable mechanistic insights.

On another note, the simulation work carried out here considered only two cation conditions, namely Li^+ and K^+ . Given that Na^+ inhibits Li^+ -mediated germination, simulations involving Na^+ could also be informative for elucidating the inhibition. To investigate possible competition between Li^+ and Na^+ , it would also be valuable in future work to perform MD simulations with both ions present. And again, in the simulations, GerAB could be present either as a monomer or within the GerA complex.

The nature of the cation interaction with receptor protein and subsequent transduction or dissipation of free energy must also be considered, particularly if the thermodynamic basis for cation-associated germination is to be established. A precedent for this can be found in the wider APC superfamily of proteins, where the specificity and activity of certain metal ion transporters is determined by disparities in binding energy associated with different cations¹⁶⁹, and perhaps similar principles apply to spore germinant receptor proteins. In this regard the observation that heat activation appeared not to influence the rate of LiCl associated germination – in contrast to the L-valine response – may be telling. One explanation for the lack of heat activation effect may be suggested by the facts that: i) heat activation is reversible, a process that is faster at higher temperatures such as 40°C ¹⁶⁰. However, since LiCl germination at 40°C is slow, reversal of heat activation during LiCl germination itself may greatly decrease effects of the initial heat activation on this germination. Or, from a thermodynamic perspective, changes in free energy upon Li^+ ion binding to the GR B-subunit protein may nullify the effects of heat activation i.e., if binding is endothermic then this could essentially cool and reverse presumed conformational changes associated with heat activation, resulting in a slow germination process. Similarly, if Li^+ binding is exothermic then this may render redundant any rate benefits conferred by the heat activation process, the dissipation of free energy upon binding providing the extra stimulus that initiates the germination process, albeit slowly, in spores with GRs that are cognate for Li^+ ions.

A number of factors then – the absence of high resolution experimental structures of any GR B-subunit proteins, a largely incomplete picture of what ‘heat activation’ entails at the molecular level, and minimal insight to the thermodynamics of ion or germinant binding – mean that we are unable to answer any of these questions with certainty at present but they do provide clear avenues for future work in this area. Ultimately, what appears at first as a biological curiosity in the field of spore

germination, happened upon by chance observation, actually invokes deeply fundamental questions concerning the underlying principles of the process. The challenge moving forward, as ever with these most intractable bacterial structures, is how best to address these.

6.5 Methods

6.5.1 Strains and spore preparation and purification

The *Bacillus* strains and species used in this work are listed in Table 3, as are the specific genotypes. Some *B. subtilis* strains had been made previously and are isogenic with the wild-type (wt) 168 strain, PS832; two other *B. subtilis* strains, PS4461 and PS4462, were described recently¹⁶⁷ and are isogenic only with each other; some additional *B. subtilis* strains are isogenic with strain PY79¹³⁰. In some cases, new strains of PS832 were made using DNA from strains carrying an antibiotic resistance marker replacing the gene(s) of interest and additional strains were made in which the antibiotic marker was removed using the Cre recombinase, all as described¹⁷⁰. Note that for the majority of the strains generated and used in this work, their genotype was validated by sequencing and subsequent analyses of the mutant strains' genomes.

In most experiments spores of *B. subtilis* strains were prepared on double strength Schaeffer's-glucose (2xSG) medium agar plates²⁷ that were incubated for 3-4 d at 37°C. The spores were then scraped from the plates and subjected to repeated washes by centrifugation with intermittent sonication, centrifuged through ~ 50% Histodenz in which spores pellet and cells and debris float, and finally Histodenz was removed by washing with water, all as described¹⁷¹. *B. megaterium* spores were prepared in supplemented nutrient broth (SNB) in a shaking (225 rpm) incubator for 72 h at 30°C and harvested and purified as described previously¹⁷². *B. cereus* spores were prepared on SNB plates at 30°C as described¹⁷³ and spores were purified by repeated washes by centrifugation, but without sonication to avoid damaging these spores' exosporium, with a final step again being centrifugation through Histodenz. All spores used in this work were >97% free of growing cells, germinated spores or obvious cell debris as determined by examination using phase contrast microscopy. Spores were stored at 4°C in water at an optical density at 600 nm (OD₆₀₀) of ~10 (~ 10⁹ spores/ml) and protected from light.

Species	Strain	Antibiotic marker	Relevant genotype	Source (ref)
<i>B. subtilis</i>	PS832	none	wild-type (wt)	Laboratory strain
<i>B. subtilis</i>	PS4461	None	wt (not PS832 background)	¹⁶⁷
<i>B. subtilis</i>	PS4462	None	PS4461 with <i>spoVA</i> ^{2mob} and <i>2duf</i>	¹⁶⁷
<i>B. subtilis</i>	PS4498	Erm	Lacks all 5 GR operons	This work
<i>B. subtilis</i>	PS4531	Erm	Lacks YrbG, Ydfr, YkjA, YdfS	¹⁶²
<i>B. subtilis</i>	FB62	Spc	Lacks GerD	¹⁷⁴
<i>B. subtilis</i>	PS4492	Km	Lacks GerA	This work
<i>B. subtilis</i>	PS4584	Erm	Lacks GerK	This work
<i>B. subtilis</i>	PS4585	Erm	Lacks GerB	This work
<i>B. subtilis</i>	PS4586	Km	Lacks YndD	This work
<i>B. subtilis</i>	PS4587	Erm	Lacks YfkQ	This work
<i>B. subtilis</i>	PS4589 ¹	none	Lacks GerA*	This work
<i>B. subtilis</i>	PS4590 ¹	none	Lacks GerK*	This work
<i>B. subtilis</i>	PS4591 ¹	none	Lacks GerB*	This work
<i>B. subtilis</i>	PS4592 ¹	none	Lacks YndD*	This work
<i>B. subtilis</i>	PS4593 ¹	none	Lacks YfkQ*	This work
<i>B. subtilis</i>	PY79	none	wt	L. Chen
<i>B. subtilis</i>	PY79	Erm	GerAB-G25A	¹³⁰
<i>B. subtilis</i>	PY79	Erm	GerAB-Y97A	¹³⁰
<i>B. subtilis</i>	PY79	Erm	GerAB-L199A	¹³⁰
<i>B. subtilis</i>	PY79	Erm	GerAB-G200A	¹³⁰
<i>B. subtilis</i>	PY79	Erm	GerAB-F342A	¹³⁰
<i>B. subtilis</i>	PY79	Erm	GerAB-triA	¹³⁰
<i>B. cereus</i>	10876	none	wt	Anne Moir
<i>B. megaterium</i>	PV361	none	plasmidless derivative of QM B1551 wt strain	Pat Vary
<i>B. megaterium</i>	GC431	Erm	pHT- <i>gerUV</i>	¹⁷²
<i>B. megaterium</i>	GC617	Km	lacks GerD; pHT- <i>gerUV</i>	¹⁷²
<i>B. megaterium</i>	GC614	Km Erm Cm Spc	lacks all 5 GR operons (<i>gers</i>)	¹⁷²

Table 3 *Bacillus* species and strains used

*The abbreviations for antibiotic resistance markers are: Erm, erythromycin (Em^r), 5 mg/ml; kanamycin (Km^r), 10-20 mg/ml; and spectinomycin (Sp^r), 100 mg/ml.

¹These strains were originally made by replacing the genes' coding regions by an antibiotic resistance marker, and then the antibiotic marker removed by the Cre recombinase.

6.5.2 Measurement of spore germination

Unless noted otherwise, *B. subtilis* spore germination used spores at an optical density at 600 nm (OD₆₀₀) of 2-5 that were heat activated in water at 70°C for 30 min, cooled on ice and used within 30-60 min. In some experiments, spores of *B. subtilis* at an OD₆₀₀ of ~ 0.5 (~ 10⁸ spores/ml) were germinated at 40°C in 200 ml with 10 mM L-valine or L-alanine, both GerA GR-dependent germinants, and in 25 mM K-HEPES buffer pH 7.4 plus ~ 50 mM TbCl₃, and Tb-DPA fluorescence was measured in duplicate at various times in a fluorometric plate reader as described (35). Germination with LiCl was at 40°C and also in 25 mM K-HEPES buffer, pH 7.4, and was much slower than L-valine germination and therefore was routinely monitored by either: i) phase contrast microscopy of ≥ 100 spores and determining the

percentages of spores that had changed from phase bright (dormant) to phase dark (fully germinated); or ii) determining the percentage of DPA release at various times by centrifuging ~ 0.5 ml samples of incubations, saving the supernatant fluid, adding 0.5 ml water to the pellet, boiling for 30 min, centrifuging and again saving the supernatant fluid. DPA in 5-, 10- and 25-ml aliquots of the two supernatants was measured in duplicate in a total of 200 ml of 25 mM K-HEPES buffer pH 7.4 and 50 mM TbCl₃ and DPA fluorescence was measured in a fluorometer. In one experiment, the effects of various concentrations of NaCl or KCl on spore germination at 40°C in 5 mM K-HEPES buffer pH 7.4 with 100 mM LiCl or L-alanine was tested.

For *B. megaterium*, germination data were collected principally via phase contrast microscopy analyses since absorbance measurements at 600 nm were compromised by clumping of spores over the duration of the experiment. Concentrated *B. megaterium* spore suspensions (OD₆₀₀ ~ 50) were heat activated at either 60°C for 10 min or 70°C for 30 min depending on the strain being examined and then cooled on ice. Spores were suspended at an OD₆₀₀ of ~ 0.4 (~ 10⁸ spores/ml) in 5 mM Tris-HCl buffer, pH 7.5, containing either 100 mM or 250 mM LiCl in a final volume of 200 µl in film-sealed 96-well plates and incubated at 30°C. Germination data were collected by analyzing phase contrast microscopy images of spore samples collected in triplicate at defined time points over 8 days. Image analysis was automated to monitor an average of ~1500 spores per strain per time point, using an ImageJ-based macro (analyze>3d objects counter>threshold 4095>size filter 20-180 pixels>exclude objects on edges>maps to show: objects> results tables to show: summary). The program calculated the total number of phase bright spores within the field of view with germinated (phase dark) spores being counted manually in order to determine the proportion of germinated spores at defined time points. An identical experimental procedure was used to examine the effect of LiCl on *B. cereus* 10876 spores.

6.5.3 Molecular Dynamics simulations of GerAB-membrane system under different ion condition

The GerAB-membrane system was prepared according to Blinker *et al*⁴⁵. GerAB structure was predicted with the template based structural prediction tool RaptorX⁶⁷, with high consensus shown with AlphaFold prediction¹⁰. The predicted structure was then used to construct a protein-membrane system with CHARMM-GUI¹³⁵ membrane builder. The bilayer membrane consists of lipid ratio of POPE, POPG and TMCL in a 1:6:3 ratio to mimic spore inner membrane. The system was solvated by TIP3P water model and including either 20 mM LiCl or 20mM KCl to neutralize the system and show comparison of system behaviour. MD simulation was carried out with GROMACS engine, version 2023.3-EasyBuild_4.9.0, with CHARMM-36 force field. The long-distance electrostatic interactions were computed by using particle mesh Ewald (PME) algorithm, and temperature was kept at 298 K with the velocity rescaling thermostat¹¹⁷ and the pressure was kept constant around 1.0 bar using the

Parrinello-Rahman barostat¹¹⁸. To remove any steric clashes and hindrances, the systems were first energy minimized using the steepest descent algorithm¹³⁷, followed by equilibration carried out according to Lee et al¹³⁵. The production runs were 1000 ns each, using a 2 fs timestep with frames saved every 2 ps. To avoid excessively large output files, trajectories were generated in segments of 100 ns each. For KCl and LiCl system, 5 parallel 1 μ s simulations were performed under identical conditions with each individual simulations initiated with different random velocities. All the production runs were carried out under periodic boundary conditions (PBC). Details of the MD simulation setup are provided in Table 4.

Cation condition of simulation systems	No. of water molecules	No. of monovalent cations	No. of Cl-ions	Temp. (K)	No. of repeats
20mM K ⁺	19336	236	6	298	5
20mM Li ⁺	19321	236	6	298	5

Table 4. Detail of MD simulations systems.

6.5.4 GerAB-cation interaction analysis

The interactions between GerAB and cations (potassium or lithium ions) during simulations were analyzed by first calculating the minimum distance between each residue and all free ions in the system for every simulation frame. An interaction was recorded when this distance dropped below the defined cutoff of 0.4 nm. The proximity between GerAB protein and cations was defined as the probability of finding a cation within 0.4 nm of a given protein residue. In addition to proximity, we also calculated the number of binding events and the average residence time as the duration of each binding event. A binding event was defined as the first frame in which the ion-residue distance dropped below 0.4 nm. The residence time was calculated as the number of consecutive frames following this event during which the ion remained within the interaction distance threshold.

6.5.5 GerAB water passage analysis

Water permeation events in simulations containing either cation were calculated following the protocol developed by our previous study¹⁴⁴. A single permeation event was defined as a water molecule continuously increasing its z-coordinate across consecutive frames, starting from the protein entrance and reaching the exit, while remaining within the region representing the protein. Events where a water molecule appeared at the entrance and exit in two consecutive frames were considered to result from periodic boundary jumps and were excluded water passage count. The entrance and exit along the z-axis were defined at $z = 2.5$ nm and $z = 7.5$ nm, respectively. The cylindrical boundary of the protein channel was defined by x and y coordinates

between 3.5 nm and 6.5 nm. As all simulations were conducted under equilibrated conditions, water was expected to permeate in both directions. Therefore, permeation events were counted in both forward and reverse directions, and the total water passage was computed by analysing all 5 simulation runs per system, each over 100 ns segments.

6.5.6 GerAB structural fluctuation analysis

The structural fluctuation of GerAB during the simulations was evaluated using multiple analyses. The overall stability of the protein was assessed by calculating the root-mean-square deviation (RMSD) and root-mean-square fluctuation (RMSF) of the carbon Alpha (CA) atoms.

6.6 Supplementary Information

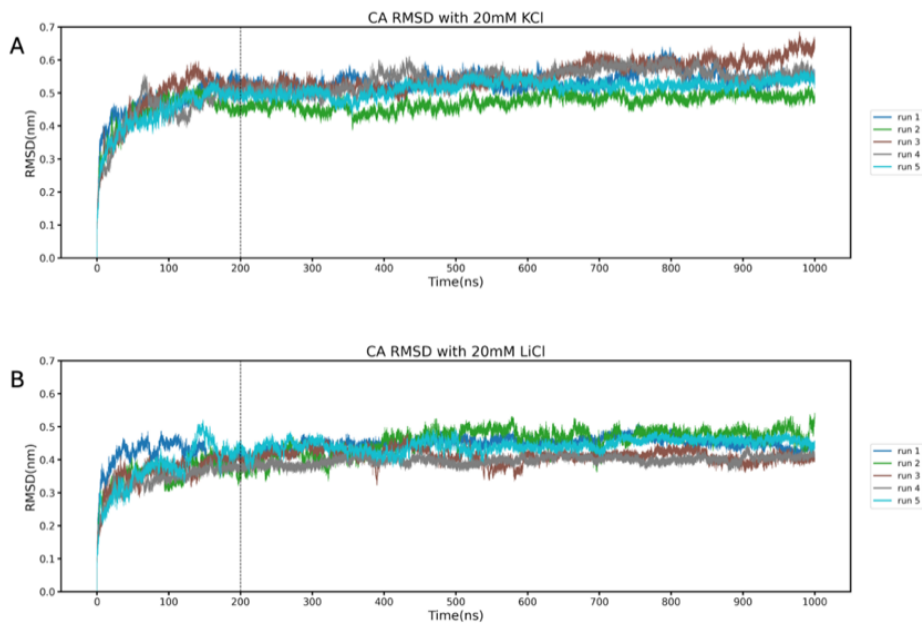


Figure S1. CA RMSD of different cation conditions tracked over simulation time. (A) CA RMSD of five parallel MD simulation runs in the presence of Li^+ . (B) CA RMSD of five MD simulation runs in the presence of K^+ . Each simulation run is represented by different colours in both panels. The dotted lines indicate the approximate time point at which the CA RMSD reached stability for all simulation runs.

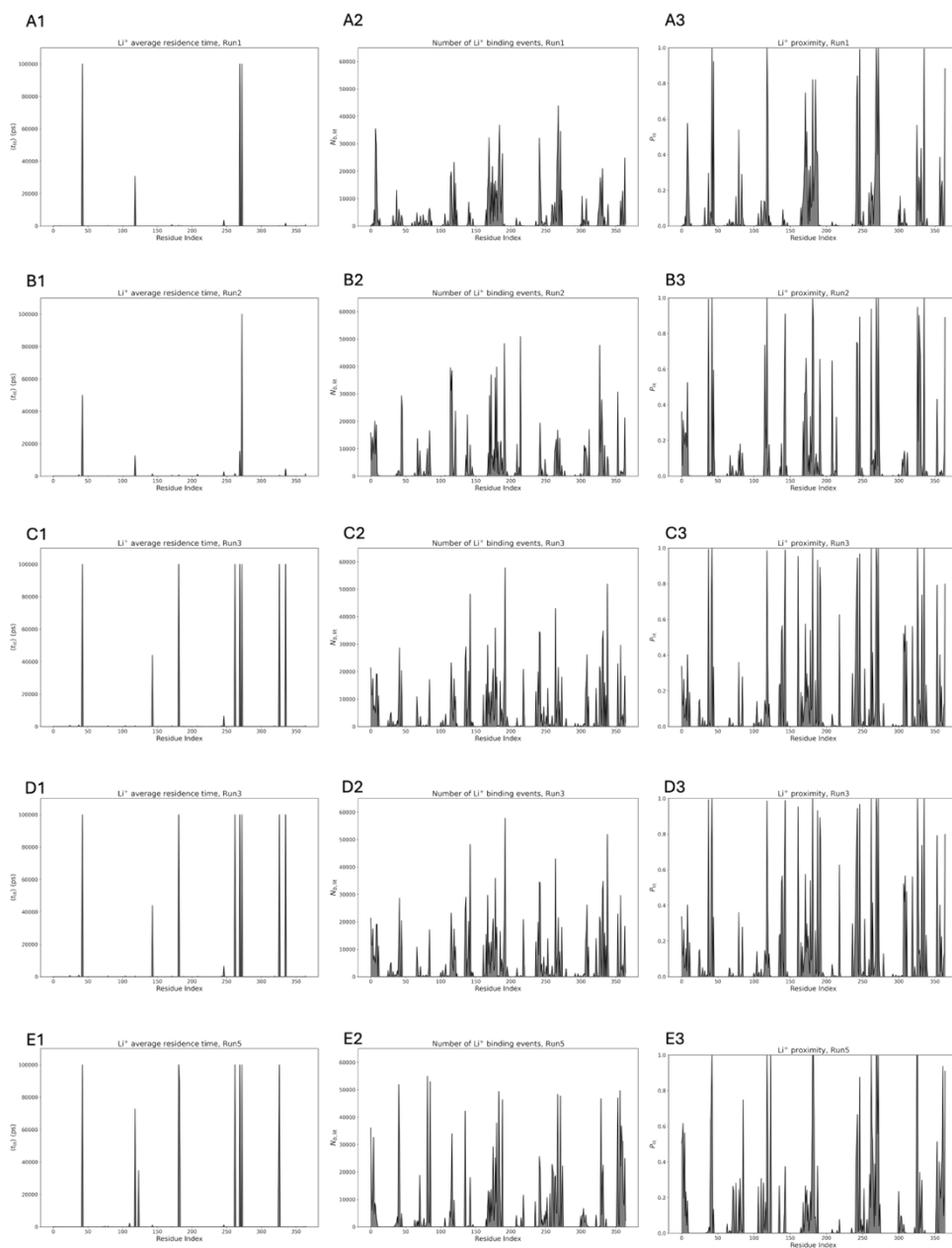


Figure S2. Li^+ interaction with GerAB across five MD simulations. Subplots A–E correspond to the five independent 1000-ns simulation runs. Subplots A1–E1: Average binding time per residue, indicating how long Li^+ remains in contact during each binding event. Subplots A2–E2: Total number of binding events between Li^+ and individual residues throughout the simulation. Subplots A3–E3: Proximity of Li^+ to GerAB residues, defined as the probability of finding a Li^+ ion within 0.4 nm of each residue.

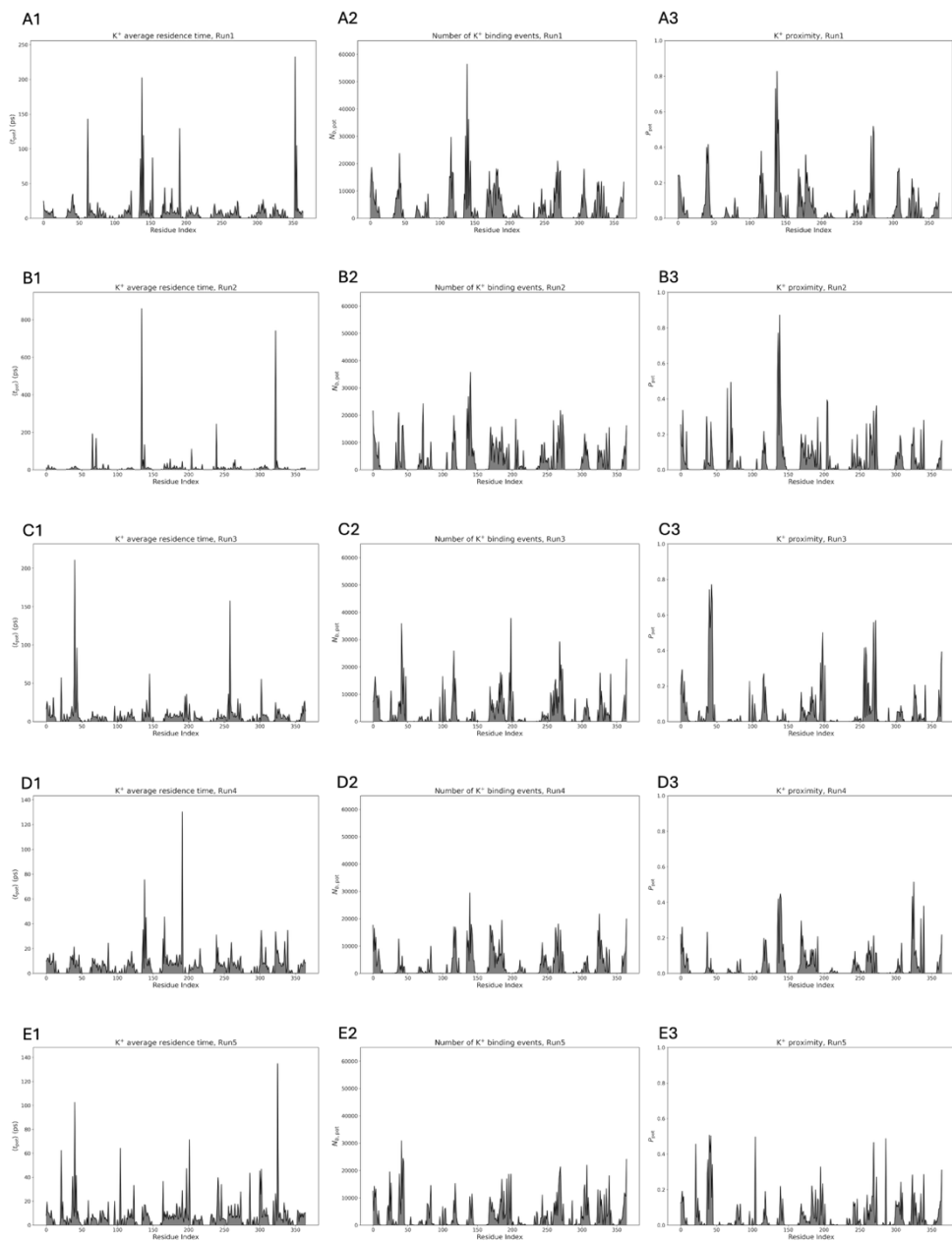


Figure S3. K⁺ interaction with GerAB across five MD simulations. Subplots A–E correspond to the five independent 1000-ns simulation runs. Subplots A1–E1: Average binding time per residue, indicating how long K⁺ remains in contact during each binding event. Subplots A2–E2: Total number of binding events between K⁺ and individual residues throughout the simulation. Subplots A3–E3: Proximity of K⁺ to GerAB residues, defined as the probability of finding a K⁺ ion within 0.4 nm of each residue.